Hydro-stochastic interpolation coupling with Budyko approach for prediction of mean annual runoff

Ning Qiu[a,b], Xi Chen[d,a,b]*, Qi Hu[c], Jintao Liu[a,b], Richao Huang[a,b], Man Gao[a,b]

[a] *State Key Laboratory of Hydrology-Water Resources and Hydraulic Engineering Hohai University, Nanjing 210098, China*
[b] *College of Hydrology and Water Resources, Hohai University, Nanjing 210098, China*
[c] *School of Natural Resources, University of Nebraska-Lincoln, Lincoln NE 68583, U.S.*
[d] *Institute of Surface-Earth System Science, Tianjin University, Tianjin China*
**Corresponding author E-mail: xichen@hhu.edu.cn*

Abstract

Hydro-stochastic interpolation method based on traditional block-kriging has often been used to predict mean annual runoff in river basins. A caveat in such method is that the statistic technique provides little physical insight on relationships between the runoff and its external forcings, such as climate and landscape. In this study, the spatial runoff is decomposed into a deterministic trend and stochastic fluctuations describing deviations from it. The former is described by the Budyko method (Fu's equation) and the latter by stochastic interpolation. The coupled method of stochastic interpolation and the Budyko method is applied to spatially interpolate runoff in the Huaihe River Basin of China, after dividing it into 40 sub-basins. Results show that the coupled method significantly improves the accuracy of predicted mean annual runoff. The error of the predicted runoff from the coupled method is much smaller than that from the Budyko method and the hydro-stochastic interpolation method. The determination coefficient for cross-validation, R_{cv}^2, from the coupled method is 0.87, larger than 0.81 from the Budyko method and 0.71 from the hydro-stochastic interpolation. Further comparisons indicate that the coupled method also has reduced error in overestimating low runoff and underestimating high runoff suffered by the other two methods. These results support that the coupled method offers an effective and accurate way to predict mean annual runoff in river basins.

Keywords: Coupled Budyko and hydro-stochastic interpolation method; mean annual runoff; prediction accuracy; Huaihe River Basin

1. Introduction

Runoff observed at the outlet of a basin is a crucial element for investigating the hydrological cycle of the basin. Because runoff is influenced by both deterministic and stochastic processes, estimating the spatial patterns of runoff and associated distribution of water resources in ungauged basins has been one of the key problems in hydrology (Sivapalan et al., 2003), and a thorny issue in water management and planning (Imbach, 2010; Greenwood et al., 2011).

In estimating and predicting runoff and regional water resources availability, we have often used regional or global runoff mapping and geostatistical interpolation method. In these methods, the value of a regional variable at a given location is estimated as a weighted average of observed values at neighboring locations. This interpolation of runoff, which is assumed as an auto-correlated generalized stochastic field (Jones, 2009), uses secondary information often referring to more than one variable (Li and Heap, 2008). Spatial autocorrelation of the runoff values is measured by the covariance or semi-variance between pairs of locations as a function of their Euclidian distance (such as in the ordinary kriging). The values obtained by the interpolation methods are the best linear unbiased estimate in the sense that the expected bias is zero and the mean squared error is minimized (Skøien et al., 2006). The ordinary kriging (OK) estimates the local mean as a constant; corresponding residuals are considered as random. Because the spatial mean could also be used as a trend or nonstationary variation in space, OK has been developed into various geostatistical interpolation methods, such as kriging with a trend by incorporating local trend within a confined neighborhood as a smoothly varying

function of the coordinates. Block kriging (BK) is an extension of OK for estimating a block value instead of a point value by replacing the point-to-point covariance with the point-to-block covariance (Wackernagel, 1995).

Unlike precipitation or evaporation which we often interpolate to find its values at specific points in space, runoff is an integrated spatially continuous process in basins (Lenton and RodriguezIturbe, 1977; Creutin and Obled, 1982; Tabios and Salas, 1985; Dingman et al., 1988; Barancourt et al., 1992; Bloschl, 2005). Streamflows are naturally organized in basins (Dooge, 1986; Sivapalan, 2005), e.g., rivers flow through sub-basins. The river network constraints water balance between upstream and downstream in a basin. The hierarchically organized river network requires that the sum of the interpolated discharge from sub-basins equals to the observed runoff at the outlet of the entire basin. Previous studies have indicated that runoff interpolation may overestimate the actual runoff without adequate information of spatial variation of runoff (Arnell, 1995), e.g., neglecting the river network in connecting sub-basins or processing basin runoff behavior as points in space (Villeneuve et al, 1979; Hisdal and Tveito, 1993). In nested basins, Gottschalk (1993a and b) developed a hydro-stochastic approach for interpolating runoff. It takes the concept that runoff is an integrated course in the hierarchical structure of river network. Distance between a pair of basins is measured by geostatistical distance instead of the Euclidian distance. The covariogram among points in conventional spatial interpolation is replaced by covariogram between basins. In this concept, runoff is assumed spatially homogeneous over basins, i.e., the expected value of runoff is a constant in space (Sauquet, 2006).

79 The observed patterns of runoff reveal systematic deviations from homogeneity
80 assumption because of influences heterogeneous rainfall among others. Meanwhile, we
81 can describe the hydrological variables of interest in deterministic forms of functions,
82 curves or distributions, and construct conceptual and mathematical models to predict
83 hydro-climate variability (Wagener et al, 2007). For example, Qiao (1982), Arnell (1992)
84 and Gao et al. (2017) used such approach and derived empirical relationships between
85 runoff and its controlling factors of climate, land-cover and topography in various basins.
86 However, the deterministic method in describing complex runoff patterns suffers
87 inevitable loss of information (Wagener et al, 2007) because of existence of uncertainty
88 in many hydrological processes and especially in observations. Thus, hydrological
89 variables also contain information of stochastic nature and should be treated as outcomes
90 from deterministic and stochastic processes. Recently, the method along this line is
91 introduced: kriging with an external drift (KED) (Goovaerts, 1997; Li and Heap, 2008;
92 Laaha et al., 2013). It accounts for deterministic patterns of spatial variables and
93 incorporates the local trend within the neighborhood search window as a linear function
94 of a smoothly varying secondary variable, instead of a function of spatial coordinates.
95 The inclusion of deterministic terms in the geostatistical methods has been shown
96 to increase interpolation accuracy of basin variables, such as mean annual runoff
97 (Sauquet, 2006), stream temperature (Laaha et al., 2013), and groundwater table
98 (Holman et al., 2009). Those deterministic terms are often described by empirical
99 formulae linking spatial features, e.g., variability of mean annual runoff in elevation
100 (Sauquet, 2006), and relationship between the mean annual stream temperature and the

altitude of gauges (Laaha et al., 2013). As a semi-empirical approach to model the deterministic process of runoff, the Budyko framework has been popularly used to analyze relationship between mean annual runoff and climatic factors, e.g., aridity index (Milly, 1994; Koster and Suarez, 1999; Zhang et al., 2001; Donohue et al., 2007; Li et al., 2013; Greve et al., 2014). Many efforts have been devoted to improving the Budyko method by including effects of other external forcing factors, such as land-use and land-cover (Donohue et al., 2007; Li et al., 2013; Han et al., 2011; Yang et al., 2007), soil properties (Porporato et al., 2004; Donohue et al., 2012), topography (Shao et al., 2012; Xu et al., 2013; Gao et al., 2017), hydro-climatic variations of seasonality (Milly, 1994; Gentine et al., 2012; Berghuijs et al., 2014), and groundwater levels (Istanbulluoglu et al., 2012). However, it has been found that use of the deterministic equation in the Budyko method alone still comes with large errors in prediction of runoff in many basins (e.g., Potter and Zhang, 2009; Jiang et al., 2015).

The aim of this study is to combine the stochastic interpolation with semi-empirical Budyko method to further improve spatial interpolation/prediction of mean annual runoff in the Huaihe River Basin (HRB), China. In this study, the spatial runoff from sub-basins in the HRB is separated into the deterministic trend and its residuals both of which are estimated by the Budyko method and interpolation method. The residuals that are calculated as difference between the observed and the estimated runoff from the Budyko method, are used in the stochastic interpolation as described in Gottschalk (1993a, 1993b, and 2000). After that, the runoff of any sub-basin is predicted as the sum of the interpolated residuals and the Budyko estimated value. The improved method is

tested in the HRB. For comparison, the leave-one-out cross-validation approach was applied to evaluate performance of the three interpolation methods: the Budyko method, hydro-stochastic interpolation, and our coupled Budyko and stochastic interpolation method.

2. Methodologies

2.1 Spatial estimation of mean annual runoff by Budyko method

The Budyko method explains the variability of mean annual water balance on a regional or global scale. It describes dependence of actual evapotranspiration (E) on precipitation (P) and potential evapotranspiration (E_0) (Williams et al., 2012). Their original relationship (E/P~E_0/P) derived by Budyko (1974) is deterministic and nonparametric. It was later developed into parametric forms (Fu, 1981; Choudhury, 1999; Yang et al., 2008; Gerrits et al., 2009; Wang and Tang, 2014). Among them, the one-parameter equation derived by Fu (Fu, 1981, Zhang et al. 2004) has been used frequently. This relationship is written

$$\frac{E}{P} = 1 + \frac{E_0}{P} - \left(1 + \left(\frac{E_0}{P}\right)^{\omega}\right)^{\frac{1}{\omega}} \quad (1)$$

or

$$R = P \cdot \left(1 + \left(\frac{E_0}{P}\right)^{\omega}\right)^{\frac{1}{\omega}} - E_0 \quad (2)$$

where, P, E, E_0, and R are mean annual precipitation, actual evapotranspiration, potential evapotranspiration, and runoff (units: mm), respectively, and ω is a dimensionless model parameter in the range of $(1, \infty)$. In these formulae, the larger the ω is, the smaller the partition of precipitation into runoff.

145 The parameter ω can be calculated using observed P, E_0, and R in gauged sub-
146 basins. The mean value of ω of a basin can be obtained by averaging ω of sub-basins,
147 or by minimizing the mean absolute error (*MAE*) in fitting the curve in Eq. (1) with
148 $E/P \sim E_0/P$ ($E = P-R$) (Legates and McCabe, 1999). Using the mean value of ω, Eq. (2)
149 can be used to predict ungauged basin runoff or to interpolate spatial variation of runoff,
150 using meteorological data in targeted sub-basins (Parajka and Szolgay, 1998).
151
152 **2.2 Hydro-stochastic interpolation method**
153 Gottschalk (1993a) described the hydro-stochastic interpolation method based on
154 the kriging method for prediction of spatial runoff. Gottschalk's method redefines a
155 relevant distance between basins, and identifies the river network and supplemental
156 water balance constraints as follows.
157 As a spatially integrated continuous process, the predicted runoff of a specific unit
158 of an area A_0 in a basin, $r^*(A_0)$, can be expressed as
159 $$r^*(A_0) = \sum_{i=1}^{n} \lambda_i r(A_i) = \Lambda^T R \quad (3)$$
160 where, $r(A_i)$ is the observed runoff in a gauged basin i with an area A_i ($i = 1, \ldots n$,
161 n is the total number of gauged basins), λ_i is the weight of basin i, Λ is the
162 transposed column vector of the weights, and R is the column vector of runoff $r(A_i)$.
163 Because $r^*(A_0)$ is an estimate of the true value $r(A_0)$, the best linear unbiased
164 estimate should satisfy $E[\, r^*(A_0) - r(A_0)\,] = 0$, where E is the expected value. If the
165 runoff is taken as a point process at the location of interest u_0, the following set of
166 equations has been developed to solve for the optimal weights under the second order

167 stationary assumption for hydrologic variables (Ripley, 1976),

168 $$\begin{cases} \sum_{j=1}^{n} \lambda_i Cov(u_i, u_j) + \mu = Cov(u_i, u_0), & i,j = 1,2,\ldots,n \\ \sum_{i=1}^{n} \lambda_i = 1\,. \end{cases} \quad (4)$$

169 In (4), $Cov(u_i, u_j)$ is the theoretical covariance function between each pair of gauged
170 stations (i=1,…, n, j=1,2…, n), $Cov(u_i, u_0)$ is the theoretical covariance of runoff
171 between the location of interest u_0 and each of the gauged stations u_i, and μ is the
172 Lagrange multiplier. After calculating the weights, λ_i, and substituting them into Eq.
173 (3), we can solve for $r^*(A_0)$.

174 According to Sauquet et al. (2000), a basin consisting of n sub-basins with areas A_j
175 (j = 1, ..., n) and observations of runoff can be further divided into M non-overlapping
176 sub-basins with areas ΔA_i. Those M sub-basins can be used as the fundamental units in
177 hydro-stochastic interpolation. The sum of the interpolated runoff for each non-
178 overlapping sub-basin should be equal to the observed runoff at the river outlet.

179 This constraint can be written as

180 $$R_T = \sum_{i=1}^{M} \Delta A_i \, r(\Delta A_i) \quad (5)$$

181 where, R_T is the streamflow observed at the outlet of the basin, ΔA_i is the non-
182 overlapping area of sub-basin i, $r(\Delta A_i)$ is the runoff depth for sub-basin i (i =
183 1, … , M). The runoff prediction for each ΔA_i is a linear combination of weights and
184 runoff observations in the n sub-basins, i.e., $r(\Delta A_i) = \sum_{j=1}^{n} \lambda_j^i r(A_j)$. Substituting it in
185 Eq. (5) we can get

186 $$R_T = \sum_{i=1}^{M} \Delta A_i \left(\sum_{j=1}^{n} \lambda_j^i r(A_j)\right) = \sum_{i=1}^{M} n_i a \left(\sum_{j=1}^{n} \lambda_j^i r(A_j)\right). \quad (6)$$

187 In (6), $r(A_j)$ is the runoff depth for sub-basin j (j = 1, ..., n) with discharge observations,
188 and λ_j^i is the weight (i= 1, ..., M; j= 1, ..., n).

Sauquet et al. (2000) divided a basin into n_T grids with equal area, a. The discharge data are converted into runoff depth under the assumption that the runoff distribution across each basin is uniform. Thus, $R_T = n_T a r_T$ for the runoff of depth r_T at the outlet of the basin. Further considering basin areas in the river network, Sauquet et al. (2000) derived the weight matrices and described a hydro-stochastic method to optimize the weights λ_j^i (i= 1, ..., M; j= 1, ..., n) in Eq. (6). Their interpolation is calculated simultaneously on multiple M non-overlapping sub-basins.

To develop the theoretical covariance function and weight matrices, the key step is to define the distance between pairs of sub-basins from the identified runoff hierarchical structure in the river network. Gottschalk (1993b) defined an appropriate geostatistical distance between sub-basins A and B,

$$d(A,B) = \frac{1}{AB}\int\int_{AB} ||u_1 - u_2|| du_1 du_2 \quad (7)$$

where, A and B are the areas of sub-basins A and B, respectively, u_1 and u_2 are the locations of pairs of points inside basins A and B, and du_1 and du_2 are the differential symbol of u_1 and u_2, respectively.

The theoretical covariogram, $Cov(A,B)$, is derived in a similar way as geostatistical distance by averaging the point process covariance function Cov_p

$$Cov(A,B) = \frac{1}{AB}\int\int_{AB} Cov_p(||u_1 - u_2||) du_1 du_2 \quad (8)$$

where, $Cov_p(||u_1 - u_2||)$ is the theoretical covariance function value of pairs of points in basins A and B with distance $||u_1 - u_2||$.

In Eq. (8), $d(A,B)$ is calculated based on grid division in each of the sub-basins (Sauquet et al., 2000). We can obtain the mean distance d between all possible pairs of

211 points (point at the center of a grid) in sub-basins A and B. For n sub-basins with
212 observations, there are $n(n+1)/2$ pairs of the sub-basins with mean distance d_i (i=1, …,
213 $n(n+1)/2$).

214 Corresponding to d_i, the empirical covariogram $Cov_e(d_i)$ can be calculated using
215 the runoff depth of pairs of the sub-basins. The geostatistical distances d_i are then
216 divided into fixed intervals (50 km in this study) to calculate the mean of $Cov_e(d_i)$
217 within each of the distance interval. The mean of $Cov_e(d_i)$ vs. the geostatistical
218 distances d_i is used to draw a scatter diagram of $Cov_e(d_i)$.

219 The trial-and-error fitting method is used to calibrate $Cov_p(\mathrm{d})$ in Eq. (8) to best
220 fit $Cov_e(\mathrm{d})$. Only independent sub-basins are used to calculate the covariance function
221 to avoid spatial correlation of nested sub-basins.

222

223 **2.3 Coupling stochastic interpolation with Budyko method**

224 The above stochastic interpolation procedure assumes a stationary stochastic
225 variation of runoff among sub-basins or spatial homogeneity in runoff (Sauquet, 2006),
226 despite variations in river network. For nonstationary variation of runoff resulting from
227 spatial heterogeneity in a river network, the spatial runoff can be decomposed into
228 nonstationary deterministic and stochastic components:

229 $$R(x) = R_d(x) + R_s(x). \quad (9)$$

230 In (9), $R(x)$ is runoff at location x, $R_d(x)$ is the deterministic component of the spatial
231 trend or the external drift (Wackernagel, 1995) that results in nonstationary variability in
232 space. $R_s(x)$ is the stochastic component considered to be stationary.

In this study, R in Eq. (2) is used as an external drift function in estimating the deterministic component $R_d(x)$ in all sub-basins, i.e., $R_d(x)$ in Eq. (9) is substituted in Eq. (2) by setting $R_d(x) = R$. The residuals between $R_d(x)$ and observed runoff are calculated for all gauged sub-basins. Furthermore, these residuals are interpolated for all ungauged sub-basins and set as the stochastic component $R_s(x)$ in Eq. (9) using the "residual kriging" method (Sauquet, 2006). In particular, $R_s(x)$ in Eq. (9) is replaced by $r^*(A_0)$ in Eq. (3) after setting $r^*(A_0) = R_s(x)$ for the stochastic interpolation scheme described in section 2.2. The superposition of these estimates of both components on the right-hand side in Eq. (9) yields the prediction of $R(x)$.

2.4 Cross validation

To validate this prediction procedure, we use the leave-one-out cross-validation method (Kearns, 1999). In addition, we examine and compare quantitatively the performances of our coupled model with the Budyko and the hydro-stochastic interpolation methods. The performance of each method is evaluated by the following metrics (Laaha and Bloschl, 2006):

$$MAE = \frac{1}{n}\sum_{j=1}^{n}[R(x_i) - R^*(x_i)\,] \quad (10)$$

$$MSE = \frac{1}{n}\sum_{j=1}^{n}[R(x_i) - R^*(x_i)\,]^2 \quad (11)$$

$$RMSE = \sqrt{\frac{1}{n}\sum_{j=1}^{n}[R(x_i) - R^*(x_i)\,]^2} \quad (12)$$

where, $R^*(x)$ and $R(x)$ are the predicted and observed runoff, respectively, *MAE* is mean absolute error, *MSE* is mean square error, and *RMSE* is the root-mean-square error. The determination coefficient for cross-validation is

$$R_{cv}^2 = 1 - \frac{V_{cv}}{V_{NK}} \quad (13)$$

where, V_{cv} is the mean square error (*MSE*), and V_{NK} is the spatial variance ($V_{NK} = \frac{\sum_{j=1}^{n}[R(x_i)-\bar{R}]^2}{n-1}$, in which $\bar{R}$ is the mean $R(x)$) of the runoff over all the tested sub-basins. In addition to these evaluation metrics, the prediction result is evaluated by regression analysis of the observation vs. prediction.

3. Study catchment and data

The Huaihe River Basin (HRB) – the sixth largest river basin in China, is used in evaluation of our coupled model and in comparison of it to the other two methods. HRB has a strong precipitation gradient from humid climate in the east and semi-humid in the west (Hu, 2008), and it is one of the major agricultural areas in China with the highest human population density in the country. Each year, millions of tons of water are consumed to meet the domestic and agriculture needs. Water resources per capita and per unit area is less than one-fifth of the national average. Moreover, more than 50% of the water resources is exploited, much higher than the recommended 30% for international inland river basins (Yan et al., 2011). Intense precipitation in a few very rainy months makes the region highly vulnerable to severe floods as well as droughts (Zhang et al., 2015). Thus, having the knowledge of spatial distribution of runoff is vital for water resources planning and management for the region.

Our study area is located upstream of the Bengbu Sluice in HRB and has a size of 121,000 km^2 (Fig. 1). The river network in the area is derived from data packages of the National Fundamental Geographic Information System, developed by National

277 Geomatics Center of China. HRB is divided into 40 sub-basins, according to available
278 hydrological stations with records from 1961-2000 (Fig. 2). Areas of the sub-basins vary
279 from the smallest of 17.9 km^2 to the largest of 30630 km^2. Among the 40 sub-basins, 27
280 are independent sub-basins and 13 are nested sub-basins.

281 Annual precipitation data used in this study are from 1961-2000 and are obtained
282 from a monthly mean climatological dataset at 0.5-degree spatial resolution. Those data
283 were developed at China Meteorological Administration and are accessible at:
284 http://data.cma.cn/data/detail/dataCode/SURF_CLI_CHN_PRE_MON_GRID_0.5.htm
285 l. The dataset was derived from observations at 2472 stations in China, using Thin Plate
286 Spline (TPS) interpolation method and the ANUSPLIN software. Pan evaporation data
287 at 21 meteorological stations in HRB are used to interpolate E_0 using the ordinary kriging
288 interpolation method and ArcGIS. The interpolated E_0 are used to derive the annual
289 potential evapotranspiration in the sub-basins of HRB. The statistical features of mean
290 annual precipitation (P), E_0 and runoff depth (R) from 1961-2000 are summarized in
291 Table 1. They show that P varied between 638-1629 mm, annual temperature between
292 11-16℃, and the mean annual E_0 between 900-1200 mm. Sub-basins in the north, e.g.,
293 ZM, ZQ, XY and ZK in Fig. 2, are relatively dry with the dryness index (E_0/P) above
294 1.3. Sub-basins in the south, e.g., MS, HBT and HC, are wetter with dryness index below
295 0.8. The average mean annual R is about 400 mm, fluctuating from a minimum of 90
296 mm in the north to a maximum of 1000 mm in the south. The temporal and spatial
297 variation in runoff is relatively small in the south and large in the north.
298
299 **4 Results**

300 **4.1 Prediction of runoff by Budyko method**

301 Actual evapotranspiration E is estimated using long-term mean annual water
302 balance (E=P-R) from 1961–2000 at the 40 sub-basins, and the results are shown in
303 Table 1. Also in Table 1 are the calculated ω values for the sub-basins. They vary from
304 1.43 of the sub-basin HWH to 3.16 of JJJ. The average of ω is 2.32 for the 40 sub-basins.
305 The comparison E/P vs. E_0/P is shown in Fig. 3. The best fit (curve) for E/P vs. E_0/P, or
306 R vs. E_0/P, is also shown in Fig, 3; it gives an alternative for average ω of the sub-basins.
307 The fitted value of ω for the 40 sub-basins determined from this process is 2.213, very
308 close to that calculated directly from the 40 individual sub-basins.

309 Using ω=*2.213* in HRB, Fu's equation in Eq. (2) can be written as

310 $$R = P \cdot \left(1 + \left(\frac{E_0}{P}\right)^{2.213}\right)^{\frac{1}{2.213}} - E_0. \quad (14)$$

311 Eq. (14) and Fig. 3 clearly show the deterministic trend of runoff in the study basin.
312 According to the water limit criterion, $E = P$, and the energy limit line criterion, $E = E_0$,
313 in Fig. 3a, the smaller the index $\frac{E_0}{P}$ is the smaller the $\frac{E}{P}$ will be (Fig. 3a) or the larger
314 the runoff will be (Fig. 3b) from the sub-basins in HRB. In Figs. 3b and 3c, the lower R
315 in the northern sub-basins indicates drier conditions (E_0/P>1.4), while the higher R in
316 the southern sub-basins assures wetter conditions (E_0/P<0.8).

317 Using P and E_0 given in Table 1 for the 40 sub-basins, we predicted runoff R by Eq.
318 (14), the Budyko method, and the deviation of the prediction from the observation. The
319 results are summarized in Tables 1 and 2. The *MAE* of predicted R is 94 mm, and *RMSE*
320 is 112 mm. The largest absolute error is in sub-basin HWH (328 mm), and the smallest
321 in sub-basin XX (24 mm). The largest relative error is 81.6% of the observed runoff in

322 sub-basin XZ, and the smallest is 5.0% of the observed runoff in XHD. They represent
323 absolute errors of 91 and 37 mm in those two sub-basins, respectively.
324
325 **4.2 Runoff from the hydro-stochastic interpolation method**
326 For comparison, the observed runoff was used in the hydro-stochastic interpolation
327 following the procedure detailed in section 2.2. In order to obtain the distance d
328 between the pairs of sub-basins, the study area is divided into 40 row × 50 column.
329 According to Eq. (7), the geostatistical distance between any two sub-basins, A and B,
330 is calculated by averaging the distances between all pairs of grid points in sub-basins A
331 and B (all the possible pairs of sub-basins are 40×41/2 for the 40 sub-basins in this study).
332 According to the estimated distance for pairs of sub-basins and the observed runoff at
333 the 40 sub-basins (Table 1), the empirical covariance $Cov_e(d)$ is estimated for each
334 pair of the sub-basins. From plots of the mean $Cov_e(d)$ of the independent sub-basin
335 pairs vs. the corresponding distance d with an interval of 50 km, we get an empirical
336 covariogram that is shown in Fig. 4. The theoretical covariance function $Cov_p(d)$ fitting
337 to the empirical covariogram is determined
338 $$Cov_p(d) = 6 \times 10^5 \exp(-d/28.62). \quad (15)$$
339 This function is further used to calculate the average theoretical covariances $Cov(A,B)$
340 in Eq. (8). Finally, the weight matrices are determined using our program in MatLab.
341 The interpolated runoff depth (R) over the 40 sub-basins along with the deviations
342 from the observation are shown in Table 1. The *MAE* and *RMSE* of R are 103 and 140
343 mm, respectively. The largest absolute and relative error is in the sub-basin JZ (401 mm

344 and 68.8%), and the smallest is in DPL (1 mm and 0.3%) (Table 2). These results indicate
345 that the errors from this interpolation method are in general larger than those from the
346 Budyko method, suggesting that the observed runoff is more influenced by the
347 deterministic trend in the basin.
348
349 **4.3 Hydro-stochastic interpolation with Fu's equation (our coupled method)**
350 We use Fu's equation, Eq. (2), to evaluate the deterministic trend or the external drift
351 function $R_d^*(x)$, and deviation of the trend from the observation, $R_s^*(x)$, assuming a
352 spatially auto-correlated process. The $R_s^*(x)$ is then used in the stochastic interpolation.
353 The empirical residual covariogram of $R_s^*(x)$ for each pair of sub-basins vs. sub-
354 basin distance is shown in Fig. 5. From the result in Fig. 5a, we obtain the exponential
355 function for $Cov_p(d)$
356 $$Cov_p(d) = 13030\exp(-d/23.9). \quad (16)$$
357 From Eq. (16), weight matrices of runoff deviation are determined by Eq. (4) using our
358 program in MatLab. They are then used to predict runoff deviation. The scatterplot of
359 the predicted residuals vs. the observed residuals shown in Fig. 5b delineates a positive
360 correlation between the predicted and the observed residuals. However, the large scatter
361 indicates limited performance by the residual model alone. Because this interpolation
362 scheme represents the spatial runoff deviation, the sum of the interpolated runoff
363 deviation and the simulated runoff by Fu's equation is the total interpolated runoff in the
364 sub-basins.
365 The predicted runoff using this procedure is given in Table 1, with the *MAE* at 71

366 mm and *RMSE* at 93 mm over the 40 sub-basins. The largest absolute error is in the sub-
367 basin QL (220 mm) and the smallest in ZM (4 mm) (Table 2). The largest relative error
368 is 47.2% of the observed runoff in XZ, and the smallest is 1% of the observed runoff in
369 sub-basin BLY. They represent absolute error of 52 and 8 mm, respectively.
370
371 **4.4 Comparisons of predicted runoff by the three methods**
372 Comparing the results summarized in Table 2, we find that our coupled method of
373 the deterministic and stochastic processes substantially reduces the runoff prediction
374 error in HRB. The *MAE* and *RMSE* of the runoff from our coupled method are much
375 smaller than those from the Budyko and the hydro-stochastic interpolation methods. In
376 cross-validation (Table 2), our coupled method has R_{cv}^2=0.87, larger than 0.81 and 0.71
377 from the Budyko method and the hydro-stochastic interpolation, respectively. The errors
378 in runoff at the sub-basins are significantly reduced. The error in HWH is 216 mm from
379 the coupled method, compared to 328 mm from the Budyko method and 300 mm from
380 the hydro-stochastic interpolation. The error in JZ is 120 mm from the coupled method,
381 compared to 179 mm from the Budyko method and 401 mm from the hydro-stochastic
382 interpolation.
383 Our correlation analysis between predicted and observed *R* is shown in Fig. 6. The
384 predicted runoff from our coupled method is highly correlated with the observed
385 (R^2=0.87). In contrast, R^2=0.82 and 0.79 for the Budyko method and the hydro-stochastic
386 interpolation, respectively. Our analysis indicates that the latter two methods
387 overestimate low runoff and underestimate high runoff, as indicated by large departures

388 from 1:1 line in Fig. 6. Similar large deviation of the runoff predicted by the hydro-
389 stochastic interpolation has also been reported by Sauquet et al. (2000), Laaha and
390 Bloschl (2006), and Yan et al. (2011).

391 Spatial distributions of runoff in the HRB calculated from the three methods are
392 shown in Fig. 7. They again show significant differences. Compared to the result from
393 our coupled method (Fig. 7c), the Budyko method overestimates runoff in most of
394 northern sub-basins (Fig. 7a), where climate is relatively dry and runoff is small (ranging
395 from 140-280 mm). The hydro-stochastic interpolation method underestimates runoff in
396 some southern sub-basins (Fig. 7b), where wet climate has fostered extremely high
397 runoff (800~1100mm) in HWH, BLY, and ZC (Table 1). The results from our coupled
398 method are closest to the observed distribution of runoff among the three methods (Fig.
399 7d). Compared to the errors in predicted runoff by the Budyko method and hydro-
400 stochastic interpolation (Fig. 7 and Table 1), our coupled method reduces the error in 70%
401 of all the sub-basins (28 of the 40 sub-basins).

402

403 **5. Discussions and conclusions**

404 In this study, we use the Budyko's deterministic method to describe mean annual
405 runoff, which is an integrated spatially continuous process and determined by both the
406 hydro-climatic elements and the hierarchical river network. A deviation from the Budyko
407 estimated runoff is used by the stochastic interpolation that assumes spatially auto-
408 correlated error. The deterministic aspects of runoff described in Budyko method are
409 reflected in regional trends at locations (sub-basins), and deviations from the trends

410 caused by stochastic processes are taking into account by the weights as a function of
411 autocorrelation and distance. Weights are larger for near points/basins and smaller for
412 distant points/basins. Information from both the Budyko method and the stochastic
413 interpolation are integrated in our coupled method to predict the runoff.

414 We have tested this coupled method and compared its results to the Budyko method
415 and the hydro-stochastic interpolation in the Huaihe River basin (HRB) in China. Our
416 results show that the deterministic process strongly affects spatial variations in runoff
417 over the 40 sub-basins in HRB. By coupling the deterministic and the stochastic
418 interpolation, our coupled mothed outperforms the Budyko method and the stochastic
419 interpolation and significantly increases the runoff prediction accuracy. The *MAE* of
420 predicted runoff over the 40 sub-basins in HRB by our coupled method is reduced to
421 71mm from 94 mm in the Budyko method and 103 mm in the stochastic method; *RMSE*
422 is reduced to 93 mm from 112 mm in the Budyko method and 140 mm in the stochastic
423 method. The largest error in predicted runoff in the HRB, in the sub-basins HWH and
424 JZ, is also substantially reduced. The runoff error in HWH is reduced to be 216 mm in
425 our coupled method from 328 mm in the Budyko method and 300 mm in the stochastic
426 method. Similarly, the runoff error in sub-basin JZ is reduced to be 120 mm in the
427 coupled method from being 179 mm in the Budyko method and 401 mm in the hydro-
428 stochastic method. The cross-validation results show that the deterministic coefficient
429 R_{cv}^2 in our coupled method is 0.87, larger than 0.81 and 0.71 in the Budyko and the
430 hydro-stochastic interpolation method, respectively. Furthermore, for high and low
431 runoff in sub-basins of HRB our coupled method gives more accurate predictions.

While substantial progress has been made by our coupled method, its results show that more effort is needed to further improve the accuracy of runoff prediction. For example, runoff prediction errors remain large from our coupled method in some sub-basins. In sub-basins MS, QL, HWH, and HNZ, the absolute error of predicted runoff is larger than 150mm and relative error of predicted runoff is larger than 20% of the observed runoff. In sub-basins BGS and XZ, the relative error of predicted runoff is larger than 40% of the observed runoff. Such large errors are largely attributed to large prediction errors intrinsic to the Budyko method (e.g., MS, QL, HWH, and XZ in Table 1). Possible causes to the errors could be from additional external factors influencing the runoff, such as land-cover, soil properties, hydro-climatic variations and groundwater. Including some or all these effects to improve the Budyko method or incorporating these effects as secondary information (e.g., multi-collocated co-kriging) will aid our understanding of the deterministic processes and help increase runoff prediction accuracy by our coupled method.

Acknowledgement

We thank the editor Erwin Zehe, the reviewers M. Mälicke and J.O. Skøien for their comments and suggestions that helped improve this manuscript substantially. The research was supported by the National Natural Science Foundation of China (No. 51190091 and 41571130071). Qi Hu's contribution was supported by USDA Cooperative Project NEB-38-088.

References

Arnell., N. W.: Factors controlling the effects of climate change on river flow regimes in a humid temperate environment, Journal of hydrology, 132(1-4), 321-342, 1992.

Arnell, N. W.: Grid mapping of river discharge. J. Hydrol., 167, 39-56, 1995.

Barancourt, C., Creutin, J. D., and Rivoirard, J.: A method for delineating and estimating rainfall fields, Wat. Resour. Res., 28, 1133-1144, 1992.

Berghuijs, W. R., Woods, R. A., and Hrachowitz, M.: A precipitation shift from snow towards rain leads to a decrease in streamflow, Nature Clim. Change, 4(7), 583–586, 2014.

Bishop, G. D., Church, M. R., Aber, J. D., Neilson, R. P., Ollinger, S. V., and Daly, C.: A comparison of mapped estimates of long term runoff in the northeast United States, Journal of Hydrology, 206: 176-190, 1998.

Bloschl, G.: Rainfall-runoff modelling of ungauged catchments, Article 133, in: Encyclopedia of Hydrological Sciences, edited by: Anderson, M. G., pp. 2061–2080, Wiley, Chicester, 2005.

Bloschl, G., Sivapalan, M., and Wagener T.: Runoff Prediction in Ungauged Basins: Synthesis Across Processes, Places and Scales, Cambridge Univ. Press, Cambridge, U. K, 2013.

Budyko, M. I.: Climate and Life, Academic, New York, 1974.

Choudhury, B.: Evaluation of an empirical equation for annual evaporation using field observations and results from a biophysical model, J. Hydrol., 216(1–2), 99–110, 1999.

Creutin, J. D. and Obled, C.: Objective analysis and mapping techniques for rainfall fields an objective comparison, Wat. Resour. Res., 18, 413-431, 1982.

Degaetano, A. T. and Belcher, B. N.: Spatial interpolation of daily maximum and minimum air temperature based on meteorological model analyses and independent observations, Journal of Applied Meteorology & Climatology, 46(11), 1981-1992, 2006.

Dingman, S. L., Seely-Reynolds, D. M. and Reynolds, R. C.: Application of kriging to estimating mean annual precipitation in a region of orographic influence, Wat. Resour. Bull., 24, 329-339, 1988.

Donohue, R. J., Roderick, M. L., and McVicar, T. R.: On the importance of including vegetation dynamics in Budyko's hydrological model, Hydrol. Earth Syst. Sci., 11(2), 983–995, 2007.

Donohue, R. J., Roderick, M. L., and McVicar, T. R.: Roots, storms and soil pores: Incorporating key ecohydrological processes into Budyko's hydrological model, 436-437, 35–50, 2012.

Dooge, J. C. I.: Looking for hydrologic laws. Water Resources Research 22 (9), 46S–58S, (2003). Linear theory of hydrologic systems. EGU Reprint Series (Originally published in 1965), Katlenburg-Lindau, Germany, 1986.

Fu, B.: On the calculation of the evaporation from land surface (in Chinese), Sci. Atmos. Sin., 1(5), 23–31, 1981.

Gao, M., Chen, X., Liu, J., and Zhang, Z. Regionalization of annual runoff characteristics and its indication of co-dependence among hydro-climate–landscape factors in Jinghe River Basin, China. Stoch Env Res Risk A, 1-18.

Gentine, P., D'Odorico, P., Lintner, B. R., Sivandran, G., and Salvucci, G.: Interdependence of climate, soil, and vegetation as constrained by the Budyko curve, Geophys. Res. Lett., 39(19), L19404, 2012.
Gerrits, A. M. J., Savenije, H. H. G., Veling, E. J. M. and Pfister, L.: Analytical derivation of the Budyko curve based on rainfall characteristics and a simple evaporation model, Water Resour. Res., 45, W04403, 2009.
Gottschalk, L.: Correlation and covariance of runoff, Stochas. Hydrol. Hydraul., 7, 85-101, 1993a.
Gottschalk, L.: Interpolation of runoff applying objective methods, Stochas. Hydrol. Hydraul., 7, 269-281, 1993b.
Gottschalk, L., Krasovskaia, I., Leblois, E., and Sauquet, E.: Mapping mean and variance of runoff in a river basin, Hydrology and Earth System Sciences Discussions, 3(2), 299-333, 2006.
Goovaerts, P.: Geostatistics for natural resources evaluation, Oxford University Press on Demand, 1997.
Greenwood, A. J. B., Benyon, R. G., and Lane. P. N. J.: A method for assessing the hydrological impact of afforestation using regional mean annual data and empirical rainfall–runoff curves, Journal of Hydrology, 411(1–2), 49-65, 2011.
Greve, P., Orlowsky, B., Mueller, B., Sheffield, J., Reichstein, M., and Seneviratne, S. I.: Global assessment of trends in wetting and drying over land, Nat. Geosci., 7(10), 716–721, 2014.
Han, S., Hu, H., Yang, D., and Liu, Q.: Irrigation impact on annual water balance of the oases in Tarim Basin, Northwest China, Hydrol. Process, 25, 167–174, 2011.
Hisdal, H., Tveito, O. E.: Generation of runoff series at ungauged locations using empirical orthogonal functions in combination with kriging, Stochas Hydrol. Hydraul., 6, 255-269, 1993.
Hollingsworth, A., Lönnberg, P.: The verification of objective analyses: diagnostics of analysis system performance, Meteorology & Atmospheric Physics, 40(1-3), 3-27, 1989.
Holman, I. P., Tascone, D., and Hess, T. M.: A comparison of stochastic and deterministic downscaling methods for modelling potential groundwater recharge under climate change in East Anglia, UK: implications for groundwater resource management, Hydrogeology Journal, 17(7), 1629-1641, 2009.
Hu, W. W., Wang, G. X., Deng, W., and Li, S. N.: The influence of dams on eco hydrological conditions in the Huaihe River basin, China, Ecological Engineering, 33(3), 233-241, 2008.
Imbach, P. L., Molina, L. G., Locatelli, B., Roupsard, O., Ciais, P., Corrales, L., and Mahé, G.: Climatology-based regional modelling of potential vegetation and average annual long-term runoff for Mesoamerica, Hydrology Earth System Sciences, 14(10), 1801-1817, 2010.
Istanbulluoglu, E., Wang, T., Wright, O. M., and Lenters, J. D.: Interpretation of hydrologic trends from a water balance perspective: The role of groundwater storage in the Budyko hypothesis, Water Resour. Res., 48, W00H16, 2012.
Jakeman, A. J. and Hornberger, G. M.: How much complexity is warranted in a rainfall-

runoff model? Water Resources Research, 29(8), 2637-2649, 2010.
Jiang, C., Xiong, L., Wang, D., Liu, P., Guo, S., and Xu, C. Y.: Separating the impacts of climate change and human activities on runoff using the Budyko-type equations with time-varying parameters, Journal of Hydrology, 522, 326-338, 2015.
Jin, X., Xu, C. Y., Zhang, Q., and Chen, Y. D.: Regionalization study of a conceptual hydrological model in Dongjiang basin, South China, Quaternary International, 208(1–2), 129-137. 2009.
Jones, O. D.: A stochastic runoff model incorporating spatial variability. 18th world IMACS CONGRESS AND MODSIM09 International congress on modelling and simulation: interfacing modelling and simulation with mathematical and computational sciences, 157(1), 1865-1871, 2009.
Jutman, T.: Runoff, Climate, Lakes and Rivers: National Atlas of Sweden. Stockholm: SNA Publishing, 106-111, 1995.
Kearns, M. and Ron, D.: Algorithmic stability and sanity-check bounds for leave-one-out cross-validation, Neural computation, 11(6), 1427-1453, 1999.
Koster, R. D. and Suarez M. J.: A simple framework for examining the inter annual variability of land surface moisture fluxes, J. Clim., 12(7), 1911–1917, 1999.
Laaha, G. and Bloschl., G.: Seasonality indices for regionalizing low flows, Hydrological Processes, 20(18), 3851-3878, 2006.
Laaha, G., Skøien, J. O., Nobilis, F., and Blöschl, G.: Spatial prediction of stream temperatures using Top-kriging with an external drift, Environmental Modeling & Assessment, 18(6), 671-683, 2013.
Legates, D. R. and McCabe. G. J.: Evaluating the use of "goodness-of-fit" measures in hydrologic and hydroclimatic model validation, Water resources research, 35(1), 233-241, 1999.
Lenton, R. L. and Rodriguez-Iturbe, I.: Rainfall network system analysis: the optimal esimation of total areal storm depth, Wat. Resour. Res., 13, 825-836, 1977.
Li, D., Pan, M., Cong, Z., Zhang, L., and Wood, E.: Vegetation control on water and energy balance within the Budyko framework, Water Resour. Res., 49(2), 969–976, 2013.
Li, J. and Heap. A. D.: A review of spatial interpolation methods for environmental scientists, 137-145, 2008.
Luo, W., Taylor, M. C. and Parker., S. R.: A comparison of spatial interpolation methods to estimate continuous wind speed surfaces using irregularly distributed data from England and Wales, International Journal of Climatology, 28(7), 947–959, 2008.
Milly, P. C. D.: Climate, soil water storage, and the average annual water balance, Water Resour. Res., 30(7), 2143–2156, 1994.
Niehoff, D. Fritsch, U., and Bronstert, A.: Land-use impacts on storm-runoff generation: scenarios of land-use change and simulation of hydrological response in a meso-scale catchment in SW-Germany, Journal of Hydrology, 267(1–2), 80-93, 2002.
Parajka, J. and Szolgay, J. Grid-based mapping of long-term mean annual potential and actual evapotranspiration in Slovakia, IAHS Publications-Series of Proceedings and Reports-Intern Assoc Hydrological Sciences, 248, 123-130, 1998.
Porporato, A., Daly, E., and Rodriguez-Iturbe, I.: Soil water balance and ecosystem

response to climate change, Am. Nat., 164(5), 625–632, 2004.
Potter, N. J. and Zhang, L.: Inter annual variability of catchment water balance in Australia, Journal of Hydrology, 369(1), 120-129, 2009.
Qiao., C. F.: Mapping runoff isocline of Hai, Luan River basin. Hydrology, (s1), 63-66, 1982.
Ripley., B. D.: The second-order analysis of stationary point processes, Journal of applied probability, 13(2), 255-266, 1976.
Sauquet, E. Mapping mean annual river discharges: Geostatistical developments for incorporating river network dependencies, Journal of Hydrology 331, 300– 314, 2006.
Sauquet, E., Gottschalk, L., and Leblois. E.: Mapping average annual runoff: a hierarchical approach applying a stochastic interpolation scheme, Hydrological Sciences Journal, 45(6), 799-815, 2000.
Shao, Q., Traylen, A., and Zhang, L.: Nonparametric method for estimating the effects of climatic and catchment characteristics on mean annual evapotranspiration, Water Resour. Res., 48, W03517, 2012.
Sivapalan, M.: Pattern, processes and function: elements of a unified theory of hydrology at the catchment scale. In: Anderson, M. (ed.) Encyclopedia of hydrological sciences, London: John Wiley, pp. 193–219, 2005.
Sivapalan, M., Takeuchi, K., Franks, S. W., Gupta, V. K., Karambiri, H., Lakshmi, V., ... and Oki, T.: Iahs decade on predictions in ungauged basins (pub), 2003–2012: shaping an exciting future for the hydrological sciences, Hydrological Sciences Journal, 48(6), 857-880, 2003.
Skøien, J. O., Merz, R., and Bloschl., G.: Top-kriging geostatistics on stream networks, Hydrology and Earth System Sciences Discussions, 2(6), 2253-2286, 2005.
Tabios, G. Q. and Salas, J. D.: A comparative analysis of techniques for spatial interpolation of precipitation, Wat. Resour. Bull., 21, 365-380, 1985.
Villeneuve, J. P., Morin, G., Bobée, B., Leblanc, D., and Delhomme, J. P.: Kriging in the design of streamflow sampling networks, Wat. Resour. Res., 15, 1833-184, 1979.
Wackernagel. H.: Multivariate geostatistics, Berlin: Springer, 1995.
Wagener, T., Sivapalan, M., Troch, P., and Woods, R.: Catchment classification and hydrologic similarity, Geography compass, 1(4), 901-931, 2007.
Wang, D. and Tang Y.: A one-parameter Budyko model for water balance captures emergent behavior in darwinian hydrologic models, Geophys. Res. Lett., 41, 4569–4577, 2014.
Williams, C. A., Reichstein, M., Buchmann, N., Baldocchi, D., Beer, C., Schwalm, C. ... and Papale, D.: Climate and vegetation controls on the surface water balance: Synthesis of evapotranspiration measured across a global network of flux towers, Water Resources Research, 48(6), 2012.
Xu, X., Liu, W., Scanlon, B. R., Zhang, L., and Pan, M. Local and global factors controlling water-energy balances within the Budyko framework, Geophys. Res. Lett., 40, 6123–6129, 2013.
Yan, Z., Xia, J., and Gottschalk, L.: Mapping runoff based on hydro-stochastic approach for the Huaihe River Basin, China, Journal of Geographical Sciences, 21(3), 441-457, 2011.

Yang, D., Sun, F., Liu, Z., Cong, Z., Ni, G., and Lei, Z. Analyzing spatial and temporal variability of annual water-energy balance in non-humid regions of China using the Budyko hypothesis, Water Resour. Res, 43, W04426, 2007.

Yang, H., Yang, D. Z. Lei, and Sun, F.: New analytical derivation of the mean annual water-energy balance equation, Water Resour. Res., 44, W03410, 2008.

Zhang, L., Dawes, W. R. G., and Walker, R.: Response of mean annual evapotranspiration to vegetation changes at catchment scale, Water Resour. Res., 37(3), 701–708, 2001.

Zhang, L., Hickel, K., Dawes, W. R., Chiew, F. H., Western, A. W., and Briggs, P. R.: A rational function approach for estimating mean annual evapotranspiration, Water Resources Research, 40(2), 2004.

Zhang, R., Chen, X. Zhang, Z. and Shi, P.: Evolution of hydrological drought under the regulation of two reservoirs in the headwater basin of the Huaihe River, China, Stochastic environmental research and risk assessment, 29(2), 487-499, 2015.

Captions of figures:

1. Figure 1 Topography and river network of study area
2. Figure 2 Sub-basins and hydrological stations of study area.
3. Figure 3 E/P ~E_0/P, (b) R ~E_0/P for the 40 sub-basins (the solid line is the best fit function), and (c) sub-basins in the north and south of the study basin. Note: in (b) and (c), blue color indicates wetter climate in the south and yellow color indicates drier climate in the north.
4. Figure 4 Empirical covariogram ($Cov_e(d)$) from sub-basin runoff data and theoretical covariogram by fitted covariance function $Cov_p(d)$ of study area.
5. Figure 5 (a) Empirical covariogram ($Cov_e(d)$) from the residual $R_s(x)$ and theoretical covariogram by fitted covariance function $Cov_p(d)$ of study area, and (b) the scatterplot of the predicted vs. the observed residuals.
6. Figure 6 Cross validation of predicted runoff vs. observation by (a) Budyko method, (b) hydro-stochastic interpolation, (c) our coupled method, and (d) the scatterplot of the predicted vs. the observed residuals for (c). The dashed-line is 1:1.
7. Figure 7 Spatial distribution of mean annul runoff estimated from (a) Budyko method, (b) hydro-stochastic interpolation, (c) our coupled method, and (d) observation.

666 Table 1: Summary of hydro-meteorological data and predicted runoff of sub-basins in HRB.

No.	Stations	Basin area (km^2)	P (mm)	R (mm)	E_0 (mm)	E_0/P	E (mm)	Budyko method			Hydro-stochastic interpolation		Coupled method	
								ω	Predicted R (mm)	Error (mm)	Predicted R (mm)	Error (mm)	Predicted R (mm)	Error (mm)
1	CTG	3090	1012	366	932	0.92	646	2.41	399	32.85	357	8.29	442	75.89
2	XHD	1431	1517	740	974	0.64	776	2.41	777	36.94	819	78.85	785	44.21
3	SQ	3094	822	168	1024	1.25	653	2.83	248	79.29	154	14.34	189	20.40
4	MS	1970	1517	672	957	0.63	845	3.06	786	114.28	705	33.18	833	161.55
5	BGS	2730	877	225	1029	1.17	651	2.57	279	53.93	331	105.51	321	95.80
6	XC	4110	945	225	997	1.06	720	3.02	332	106.82	197	27.83	261	35.87
7	BT	11280	910	223	993	1.09	687	2.85	310	86.94	205	18.10	220	3.73
8	ZK	25800	678	123	1061	1.56	555	2.54	163	39.96	101	21.54	101	21.60
9	JJJ	5930	1347	513	969	0.72	834	3.16	640	127.27	369	143.29	555	42.76
10	HB	16005	1092	335	937	0.86	757	3.15	455	120.48	197	137.61	383	48.20
11	ZQ	3410	739	118	1083	1.47	621	2.83	190	71.71	101	17.02	125	7.56
12	HPT	4370	1629	764	984	0.60	865	2.92	868	103.53	729	34.69	896	131.58
13	XX	10190	987	367	1053	1.07	620	2.10	343	23.77	297	70.54	325	41.95
14	BB	121330	850	215	1024	1.20	635	2.54	264	49.48	71	143.43	175	39.74
15	WJB	30630	1003	294	957	0.95	709	2.85	384	90.29	225	68.43	280	14.17
16	LZ	390	963	345	1078	1.12	618	2.09	320	24.96	335	10.87	337	8.57
17	NLD	1500	1019	439	1101	1.08	581	1.86	351	88.30	350	88.75	388	50.60
18	ZMD	109	690	212	1093	1.58	478	1.94	163	48.65	265	52.90	157	54.73
19	BLY	737	1504	868	1126	0.75	635	1.69	695	173.27	783	85.32	861	7.54
20	HWH	292	1560	1068	1127	0.72	492	1.43	740	328.03	768	299.97	852	216.14
21	ZC	493	1512	838	1112	0.74	674	1.79	708	130.23	700	137.94	790	48.34
22	BQY	284	1268	693	1094	0.86	575	1.68	527	166.21	543	150.04	568	125.47
23	QL	178	1559	970	1090	0.70	589	1.60	756	214.17	749	221.28	749	220.34
24	HNZ	805	1480	640	1114	0.75	840	2.41	681	41.37	576	63.94	816	175.57
25	TJH	152	1305	699	1090	0.84	605	1.74	556	143.66	309	390.52	556	143.05
26	LX	77.8	1025	484	1079	1.05	540	1.75	361	123.77	302	182.46	368	116.82
27	ZLS	1880	755	253	1104	1.46	502	1.91	194	58.45	197	55.37	223	29.21
28	ZT	501	1021	437	1101	1.08	583	1.87	351	85.87	212	225.14	452	14.74

29	XGS	375	830	302	1088	1.31	528	1.91	238	63.74	99	202.58	317	15.33
30	JZ	46	1103	583	1107	1.00	520	1.63	404	178.81	182	401.32	463	120.48
31	GC	620	638	111	1055	1.65	528	2.51	145	34.18	53	57.92	125	14.85
32	ZM	2106	645	97	1039	1.61	548	2.72	150	53.48	72	24.71	100	3.62
33	YZ	814	979	235	1083	1.11	743	2.85	329	94.07	271	35.66	321	85.76
34	XZ	1120	746	111	1040	1.39	636	3.06	202	90.66	84	27.12	163	52.32
35	GZ	1030	855	342	1098	1.28	513	1.81	250	92.10	230	111.80	260	81.82
36	DPL	1770	1067	331	1066	1.00	736	2.57	393	61.62	330	1.02	437	105.29
37	XX2	256	1301	606	1092	0.84	695	2.00	552	53.68	708	101.78	732	126.63
38	PH	17.9	1248	708	1094	0.88	540	1.61	512	196.04	605	102.78	564	144.41
39	HC	2050	1255	454	1095	0.87	802	2.54	517	63.36	328	125.79	537	83.61
40	HK	2141	871	227	1077	1.24	644	2.44	264	37.28	273	46.15	243	16.02

667

668

669

Table 2: Interpolation cross-validation errors between the predicted and observed runoff in 40 sub-basins from the three methods.

Evaluation indicators	Budyko method	Hydro-stochastic interpolation	Coupling method
MAE (mm)	94	103	71
MSE (mm^2)	12561	19828	8557
RMSE (mm)	112	140	93
Max absolute error (mm)	328	401	220
Min absolute error (mm)	24	1	4
Max relative error (%)	82	69	47
Min relative error (%)	5	0.3	1
R_{cv}^2	0.81	0.71	0.87

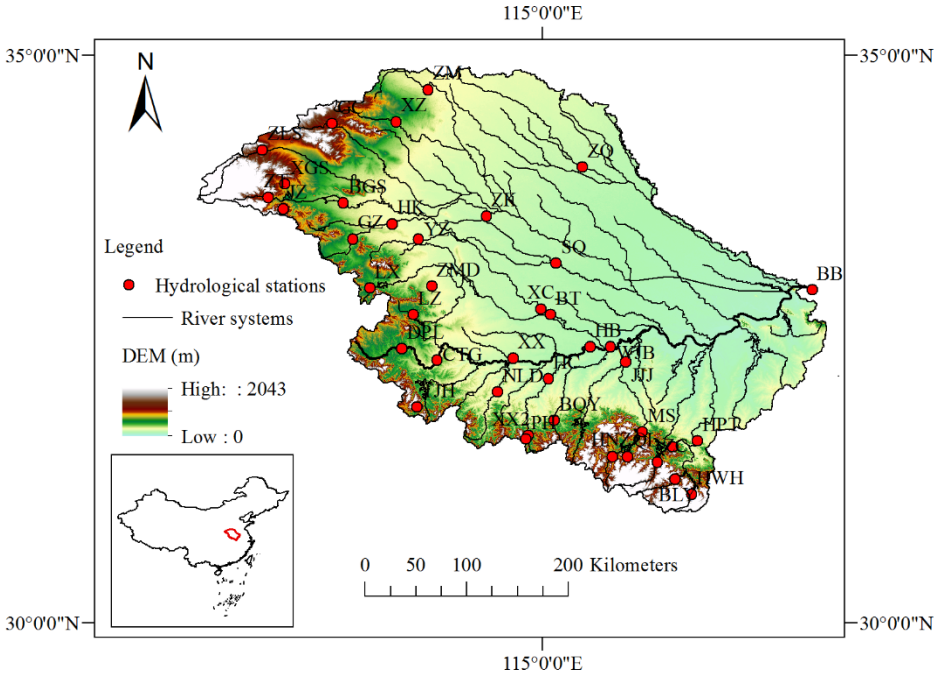

Figure 1: Topography and river network of study area.

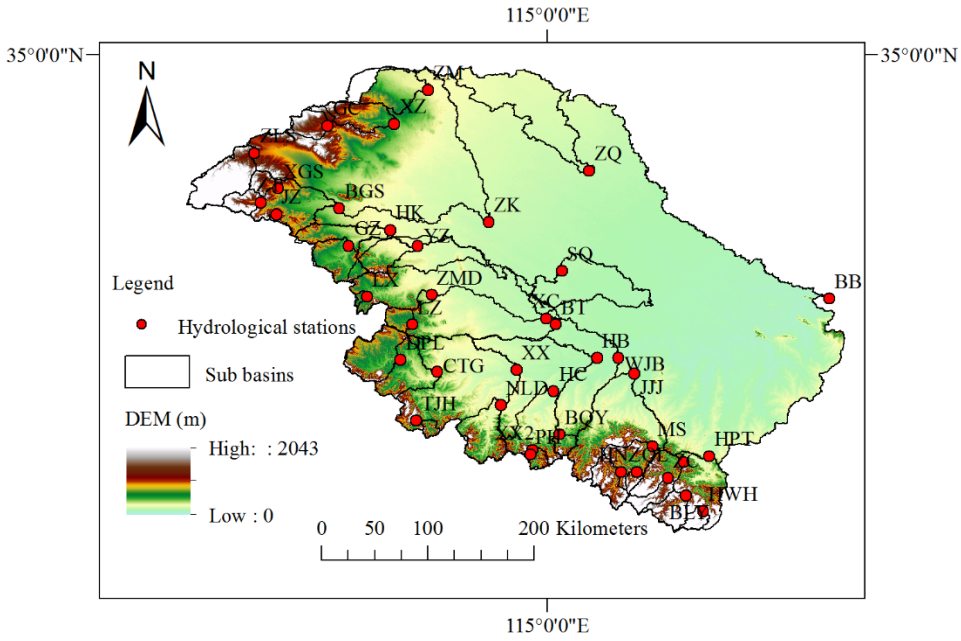

Figure 2: Sub-basins and hydrological stations of study area.

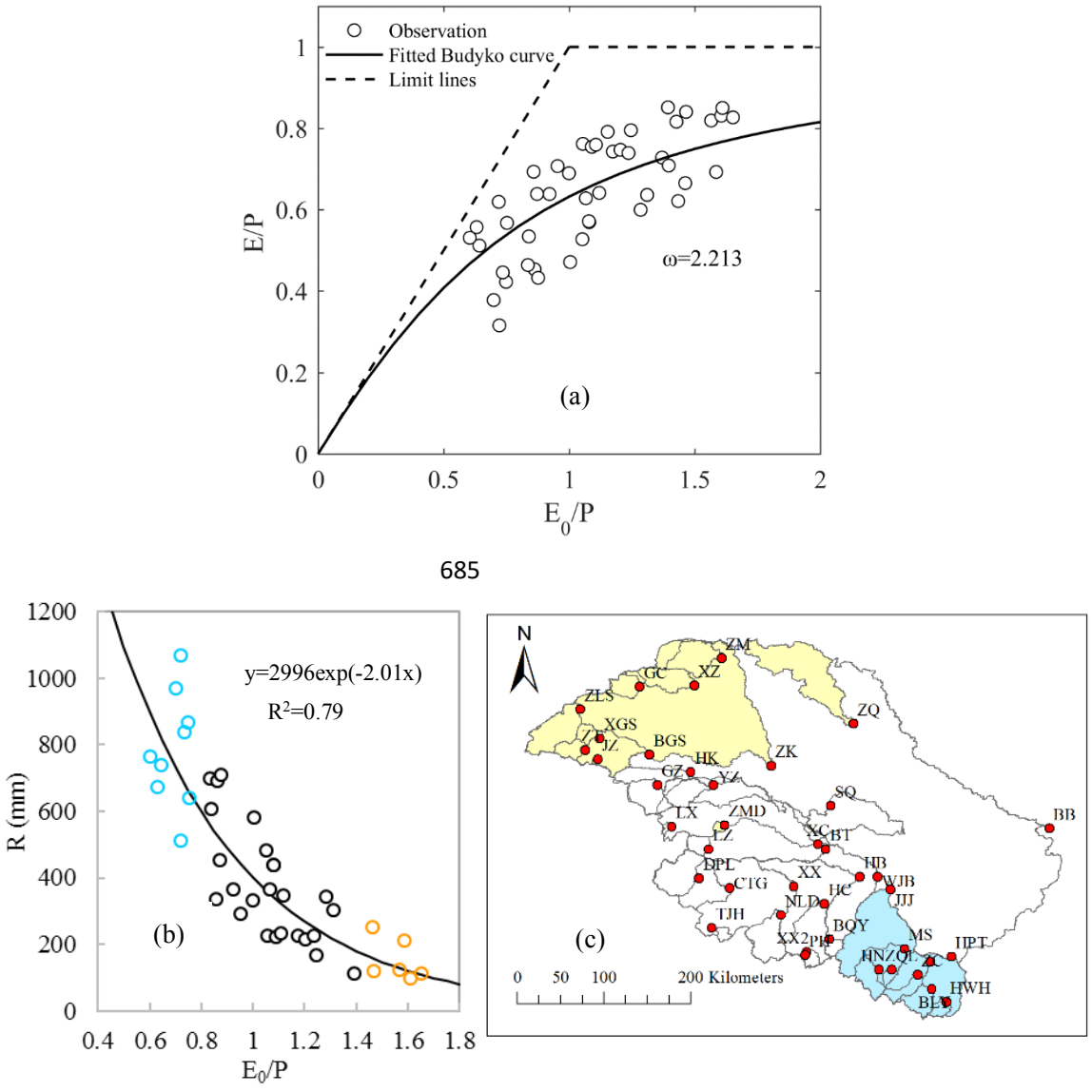

Figure 3: (a) $E/P \sim E_0/P$, (b) $R \sim E_0/P$ for the 40 sub-basins (the solid line is the best fit function), and (c) sub-basins in the north and south of the study basin. Note: in (b) and (c), blue color indicates wetter climate in the south and yellow color indicates drier climate in the north.

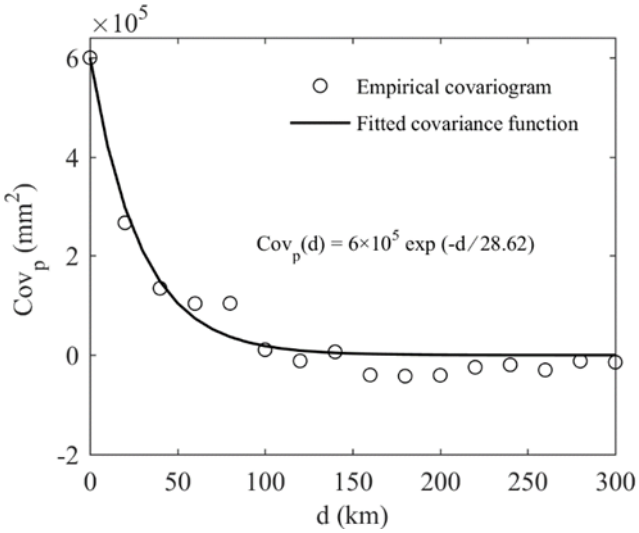

Figure 4: Empirical covariogram ($Cov_e(d)$) from sub-basin runoff data and theoretical covariogram by fitted covariance function $Cov_p(d)$ of study area.

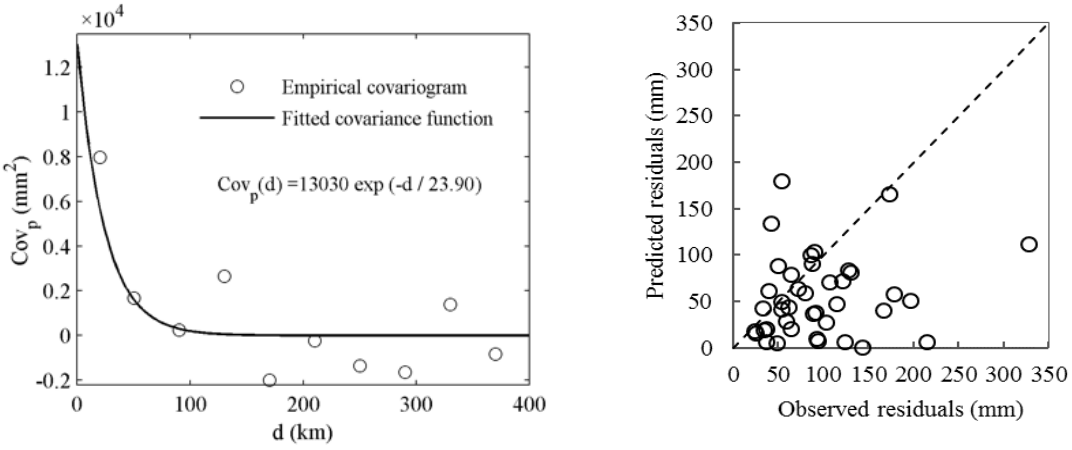

(a) (b)

Figure 5: (a) Empirical covariogram ($Cov_e(d)$) from the residual $R_s(x)$ and theoretical covariogram by fitted covariance function $Cov_p(d)$ of study area, and (b) the scatterplot of the predicted vs. the observed residuals.

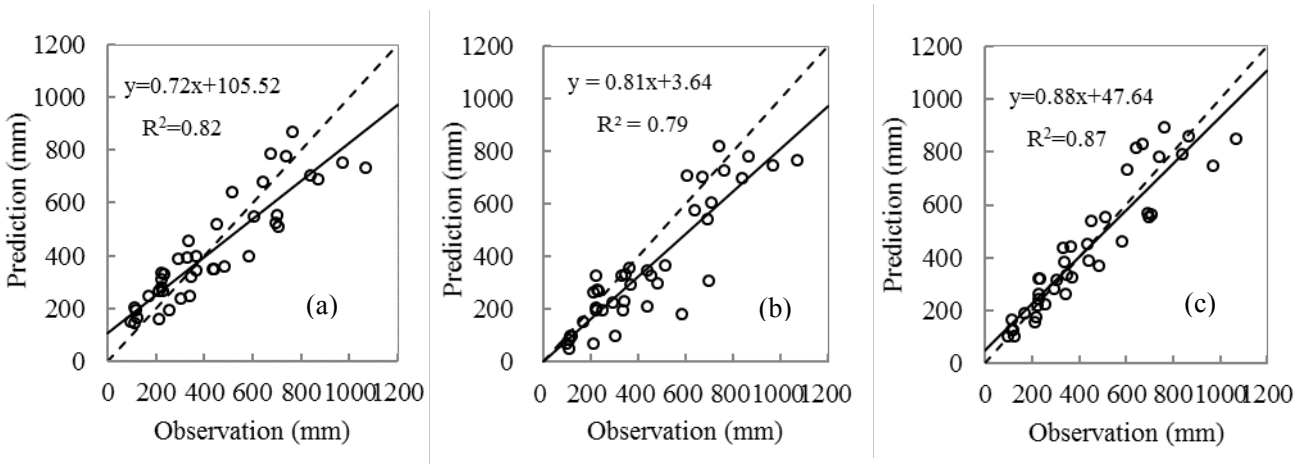

Figure 6: Cross validation of predicted runoff vs. observation by (a) Budyko method, (b) hydro-stochastic interpolation, and (c) our coupled method. The dashed-line is 1:1.

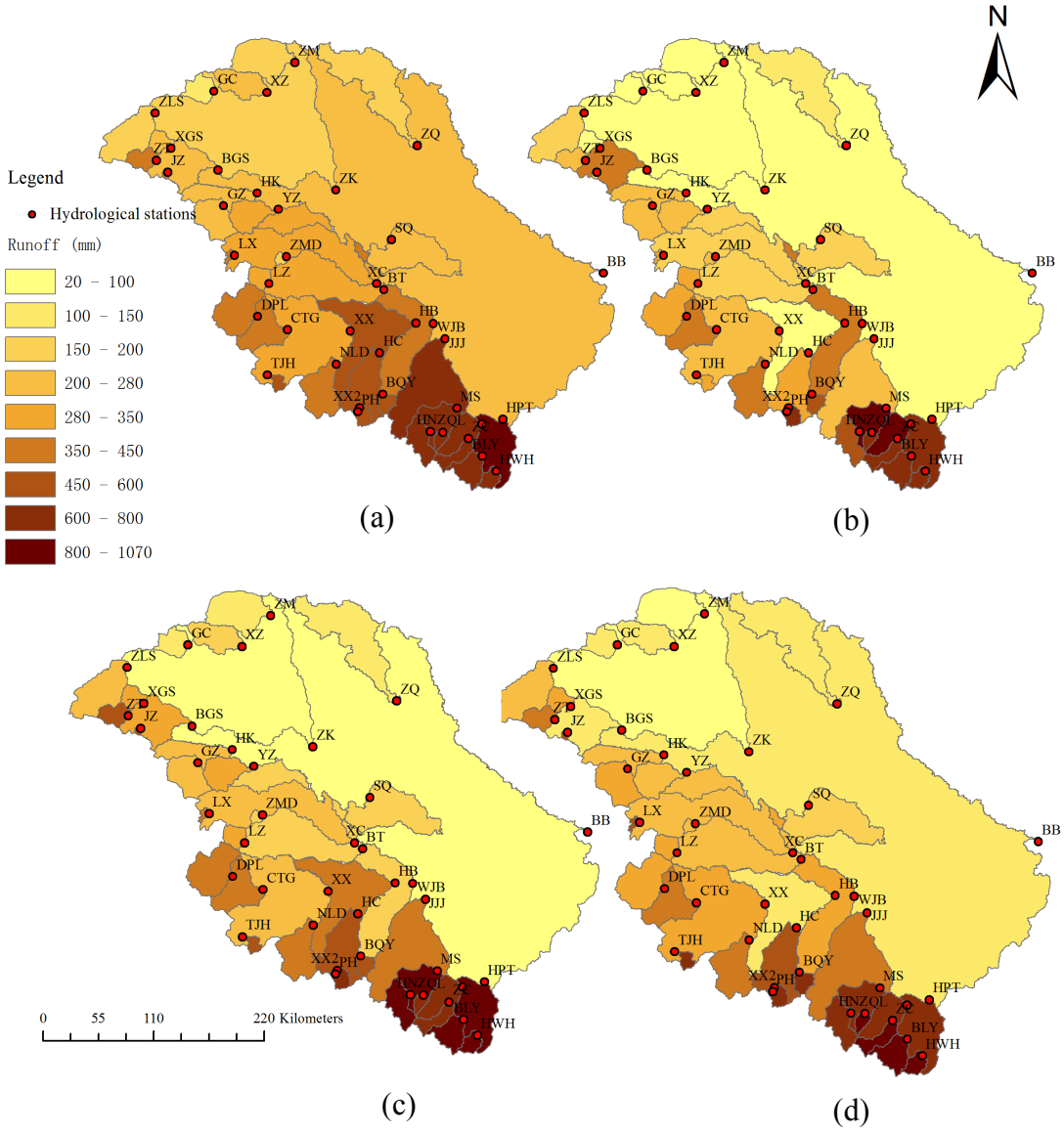

721

722

723 Figure 7: Spatial distribution of mean annul runoff estimated from (a) Budyko method, (b) hydro-

724 stochastic interpolation, (c) our coupled method, and (d) observation.

725